J Mol Model (2006) 12: 182–189
DOI 10.1007/s00894-005-0016-8

ORIGINAL PAPER

Yi Ren · Ming Li · Ning-Bew Wong · San-Yan Chu

Ab initio computational insight into the ion-pair S_N2 reaction of lithium isothiocyanate and methyl fluoride in the gas phase and in acetone solution

Received: 28 December 2004 / Accepted: 1 July 2005 / Published online: 29 October 2005

Abstract The ion-pair S_N2 reaction LiNCS + CH_3F with two mechanisms, inversion and retention, was investigated at the MP2(full)/6-311 + G**//HF/6-311 + G** level in the gas phase and in acetone solution. All HF-optimized structures were confirmed by vibrational frequency analysis. Based on IRC analyses, eight possible reaction pathways in the title reaction are proposed. The inversion mechanism through a six-membered-ring transition-state structure is the most favorable. Methyl thiocyanate should form preferentially in the gas phase and the more stable methyl isothiocyanate will be the main product in CH_3COCH_3. The retardation of the reaction in CH_3COCH_3 solution was attributed to the differences in the solvation free energies in the separated reactants and transition structures. All of the theoretical results are consistent with the experiment.

Keywords Ab initio · Thiocyanates and isothiocyanates · Ion-pair S_N2 reaction · Inversion and retention mechanisms

Y. Ren (✉) · M. Li
School of chemistry of chemical engineering, Southwest China Normal University, 400715 Chongqing, PR China
E-mail: yiren57@hotmail.com
Fax: +86-28-85257397

Y. Ren
College of Chemistry, Sichuan University, 610064 Chengdu, PR. China

N.-B. Wong
Department of Biology and Chemistry, City University of Hong Kong, Kowloon, Hong Kong

S.-Y. Chu
Department of Chemistry, National Tsing Hua University, 30013 Hsinchu, Taiwan

Introduction

Organic thiocyanates and their isomeric compounds, i.e., isothiocyanates, with an ambidextrous group –NCS or –SCN are useful for syntheses of compounds containing both sulfur and nitrogen [1–6]. Some isothiocyanates are physiologically active and occur as natural products. For example, allyl isothiocyanate $CH_2=CHCH_2NCS$ is a major component of mustard oil and horseradish root. Isothiocyanates can be prepared by thermal rearrangement of the analogous thiocyanate isomer [7], which can be obtained by treatment of alkyl halides or tosylates with alkali metal thiocyanate (Eq. 1). This is a practical route for the synthesis of organic thiocyanates and isothiocyanates [8].

$$MNCS + RX \rightarrow MX + RSCN \rightarrow MX + RNCS \qquad (1)$$

As one of the most important reactions in chemistry, the anionic S_N2 reactions at carbon have been well investigated [9–11]. However, only a few theoretical studies on ion-pair S_N2 reactions have been reported [12–16], even though some experimental results are available [17–22]. Harder et al. [12] studied some symmetric ion-pair S_N2 reactions MX + CH_3X (M = Li and Na; X = F and Cl) at the MP4/6-31 + G*//HF/6-31 + G* level. Streitwieser et al. [13] extended the work to the higher alkyls and discussed some steric effects for the ion-pair displacement reactions. Leung et al. [14] investigated the structure of alkali-metal cyanates and isocyanates and their related ion-pair S_N2 reactions. Their calculated results show that methyl cyanate should form preferentially via a six-membered-ring transition-state (TS) structure based on analysis of transition structures if the reaction involves a monomer ion-pair inversion pathway. In our recent theoretical studies on the gas phase reaction of LiNCS with CH_3F (Eq. 2), the inversion mechanism was described in detail [23]. Our results reveal that there are four possible reaction pathways and methyl thiocyanate CH_3SCN should form preferentially by a six-membered-ring TS.

$$LiNCS + CH_3F \rightarrow CH_3SCN \rightarrow LiF \rightarrow CH_3NCS + LiF \quad (2)$$

Glukhovtsev et al. [24] pointed out that the anionic S_N2 reaction of CH_3X with X^-might, at least in principle, take place by either back-side or front-side attack, leading to displacement products with inversion or retention of configuration, though the barrier for the front attack is significantly higher. Interestingly, the two reaction mechanisms, inversion and retention, involved in the ion-pair S_N2 reactions are competitive. Our previous studies on the ion-pair S_N2 reactions LiY + CH_3X (Y, X = F, Cl, Br and I) also show that the retention mechanism is favorable for the reactions involving fluorine [25].

As a part of our continued interest in the mechanism of S_N2, in the present work we will explore the retention mechanism for Eq. 2 and hope to address what is the most likely pathway. Our aim is to contribute to a better understanding of the ion-pair S_N2 reaction at carbon and to clarify the nature of all possible TS for the title reaction. We also focus on the influence of the solvent, CH_3COCH_3 in our case, in an attempt to analyze solvent effects that might produce significant effects on the reaction mechanism and lead to different products. For comparison, the differences between two mechanisms, inversion and retention, were also discussed.

Methodology

Veszprémi et al. [26] pointed out correlation energy should be included for a good description of the bonding in the structures of some pseudohalides –NCO, –NCS, and $–N_3$. In this work, the geometries of all species were fully optimized using HF/6-311 + G**. The electron correlation effect was taken into account by further single-point MP2 calculations with all electrons included in the correlation treatment, i.e., MP2(full)/6-311 + G**//HF/6-311 + G**, hereafter designated MP2(full). All HF-optimized structures were characterized by vibrational frequency calculations. Zero-point energy (ZPE) corrections with a scaling factor of 0.9248 [27] were applied to the calculated total and relative energies. Thermodynamics properties were estimated using standard procedures at 298.15 K and 1 atm (Eqs 3–5). The structures of complexes in the reaction pathways were obtained by optimization of the last structures on both sides of the IRC calculations [28, 29]. Charge distributions were obtained from the wavefunctions calculated at the MP2(full) level on the HF geometries using the natural population analysis (NPA) [30].

$$E_{thermal} = E_{vib} + E_{rot} + E_{trans} \quad (3)$$

$$H = E_{elec} + ZPE + E_{thermal} + RT \quad (4)$$

$$G = H - TS \quad (5)$$

To estimate the solvent effects on the title reaction, the polarized continuum model (PCM) [31], was used for optimization at the HF/6-311 + G** level. The solvent in the present work is a dipolar aprotic solvent CH_3COCH_3 (ε = 20.70). In the PCM procedure, the molecule is inserted in a cavity of realistic shape formed by interlocking spheres centered on solute atoms or atomic groups, and solute–solvent interactions are reproduced by means of point charges on the cavity surface. This can give very accurate solvation free energies for a large variety of compounds. The solvation stabilization energies (SSE) were calculated at the MP2(full)/6-311 + G** level on the HF/6-311 + G** geometries. All calculations were performed using the Gaussian 98 set of programs [32].

Throughout this paper, all internuclear distances are in Å and bond angles are in degrees. Relative energies (in kJ mol^{-1}) within the text correspond to enthalpy changes ($\Delta \boldsymbol{H}_{298}$) and the Gibbs free energy changes ($\Delta \boldsymbol{G}_{298}$).

Results and discussion

The energy profile for the exothermic ion-pair S_N2 reaction (Eq. 2) in the gas phase may be described by an asymmetrical double-well potential curve (Scheme 1). Initially, the reactants (**1** and **2a** or **2b**) come together to form the pre-reaction dipole–dipole complex (R-com, **3a**–**c**), with complexation energies ΔH_{comp} and ΔG_{comp}. This complex must then overcome an activation barrier that we term the central barrier, $\Delta H^{\neq}_{cent}$ and $\Delta G^{\neq}_{cent}$, to reach an inversion TS structure (Inv-TS, **4a**–**d**) or retention transition structure (Ret-TS, **4a′**–**d′**). The energy then drops with the formation of the product dipole–dipole complex (P-com, **5a**–**b**), which finally dissociates into the separated products (**6a** or **6b** and **6c**). The overall barrier, i.e., the barrier relative to separated reactants, is denoted $\Delta H^{\neq}_{ovr}$ and $\Delta G^{\neq}_{ovr}$. While ΔH_{ovr} and ΔG_{ovr} are the overall energy changes for the title reaction for the forward direction. The relative energies involved in the title reaction are summarized in Table 1 (in the gas phase) and in Table 2 (in CH_3COCH_3).

Reactants and products

The optimized geometries of lithium isothiocyanate and its isomer are shown in Fig. 1. Previous studies of Veszprémi et al. [26] indicated that there are three possible isomers formed by lithium and –NCS. Linear lithium isothiocyanate (**2b**), denoted as LiNCS(l), and a T-shaped structure (**2a**), LiNCS(T) are stable on the potential energy surface in the gas phase, but linear LiSCN does not exist. The T-shape isomer, LiNCS(T), in which a π-complex is formed between the empty orbital of lithium and the π-system of -NCS functional group, is more stable. Our results show that **2a** is lower than **2b** by 3.4 kJ mol^{-1} in terms of $\Delta \boldsymbol{H}_{298}$.

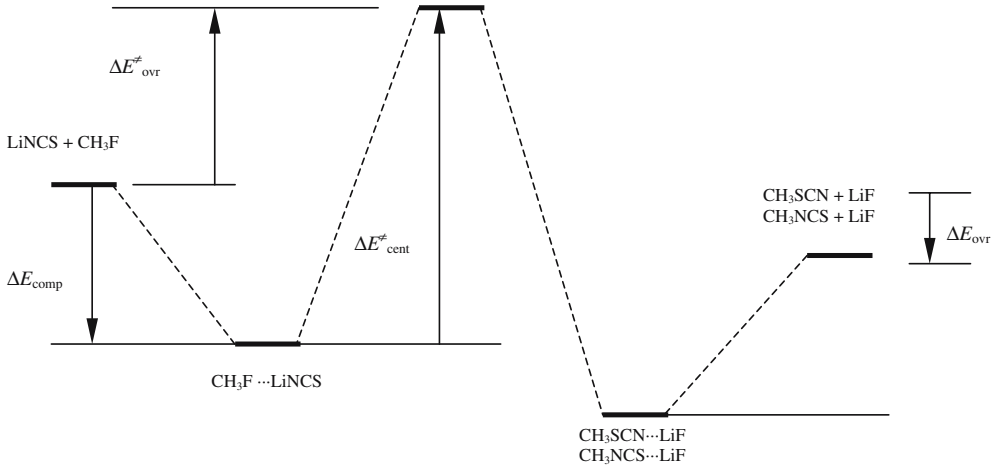

Scheme 1 Schematic potential energy profile for title reaction in the gas-phase

Calculated geometrical parameters of two products—methyl thiocyanate (**6a**) and methyl isothiocyanate (**6b**) are shown in Fig. 1. At the HF/6-311 + G** level, **6a** has a bent structure at the sulfur atom, and **6b** is linear. The latter was found to be 4.4 kJ mol^{-1} (in terms of ΔH_{298}) more stable than **6a**, similar to the isomerization of allyl thiocyanate to allyl isothiocyanate, where the isothiocyanate is lower in energy than allyl thiocyanate by > 13 kJ mol^{-1} [33].

Reactant complexes

There are three stable conformers in the gas phase for the reactant dipole–dipole complexes, **3a**–**c**, formed between CH_3F and LiNCS. All of them place the lithium cation in a complex with the halogen to form a so-called "X-philic" reactant complex CH_3F···LiNCS, in which lithium isothiocyanate keeps its T-shaped structure in **3a**-**b**, but is linear in **3c**. In forming **3a**, the incoming lithium cation strongly interacts with the fluorine ion. Meanwhile, there is a weaker interaction between the sulfur atom on the -NCS group and a hydrogen atom of the methyl group, in which the F–Li distance is 1.854 Å. In the complex **3b**, the nitrogen atom is closer to one of the hydrogen atoms on methyl group. The F–Li distance is 1.847 Å and the nitrogen is 2.712 Å from the hydrogen.

Reaction of CH_3F with LiNCS gives MP2(full) complexation energies of 65.8 kJ mol^{-1} (**3a**), 74.7 kJ mol^{-1} (**3b**) and 70.8 kJ mol^{-1} (**3c**). The shorter Li–F and N–H distances make **3b** and **3c** more stable than **3a** by about 8.9 and 5.0 kJ mol^{-1} in the gas phase, respectively.

The effects of CH_3F···LiNCS complexation are twofold: (1) it increases the C–F bond distance in the free reactants from 1.365 to about 1.41 Å in **3a**–**c**. (2) it increases the effective positive charge on the CH_3 group in the complex H_3CF···LiNCS from +0.43*e* to +0.50*e* (**3a**–**c**), which is favorable for the subsequent nucleophilic attack.

TS structures

Four transition structures (**4a**–**d**) were found for the reaction of LiNCS with CH_3F with the inversion mechanism [23], in which the nucleophilic site (N or S) attacks the central carbon from the back-side. Two of them (**4a** and **4c**) involve a planar six-membered ring structure. The remaining two (**4b** and **4d**) are four-membered rings. Four other TS structures, **4a′**–**d′**, were located if the reaction follow the retention mechanism. In these retention TS structures, the nucleophilic site attacks methyl fluoride from the front-side of the central carbon atom and the leaving group and nucleophile are on the same side of the CH_3 moiety. One nucleophilic site (N) of the isothiocyanates coordinates with lithium, and the other (S) attacks methyl fluoride, leading to a planar six- membered ring TS structure (**4a′**). In another planar six-membered-ring TS structure **4c′**, the nucleophilic site (S) of the isothiocyanate coordinates with lithium, and the other (N) attacks methyl fluoride. If the same sulfur atom (S) on the T-shape LiNCS moiety or nitrogen atom (N) on the linear LiNCS moiety coordinates with lithium and attacks methyl fluoride from the front-side simultaneously, four-membered-ring TS structures (**4b′** and **4d′**) are formed.

The gas phase overall reaction barriers for back-side attack with inversion of configuration and for front-side attack with retention of configuration are given in Table 1. Table 1 reveals that the overall barriers,$\Delta H^{\neq}_{298}$(gas), for the title reaction increases in the following order: 70.0(**4a**) < 120.5 (**4c**) < 159.6 (**4a′**) < 162.3(**4d′**) < 176.8(**4c′**) < 183.3(**4b′**) < 214.4(**4d**) < 254.0(**4b**) kJ mol^{-1}. Contributions of $-T\Delta S^{\neq}$ to the Gibbs free energy of activation, $\Delta G^{\neq}_{298}$(gas), are relatively large, and $-T\Delta S^{\neq}$ is 16.9%(**4d**) ~ 63%(**4a**) of $H^{\neq}_{298}$(gas). The barriers in terms of $\Delta G^{\neq}_{298}$(gas) follow the same order: 113.9(**4a**) < 165.8 (**4c**) < 195.9(**4a′**) < 197.4(**4d′**) < 214.5(**4c′**) < 221.6(**4b′**) < 250.6(**4d**) < 299.0(**4b**) kJ mol^{-1}. This indicates that the retention barriers for the six-membered-ring TS structures **4a′** and

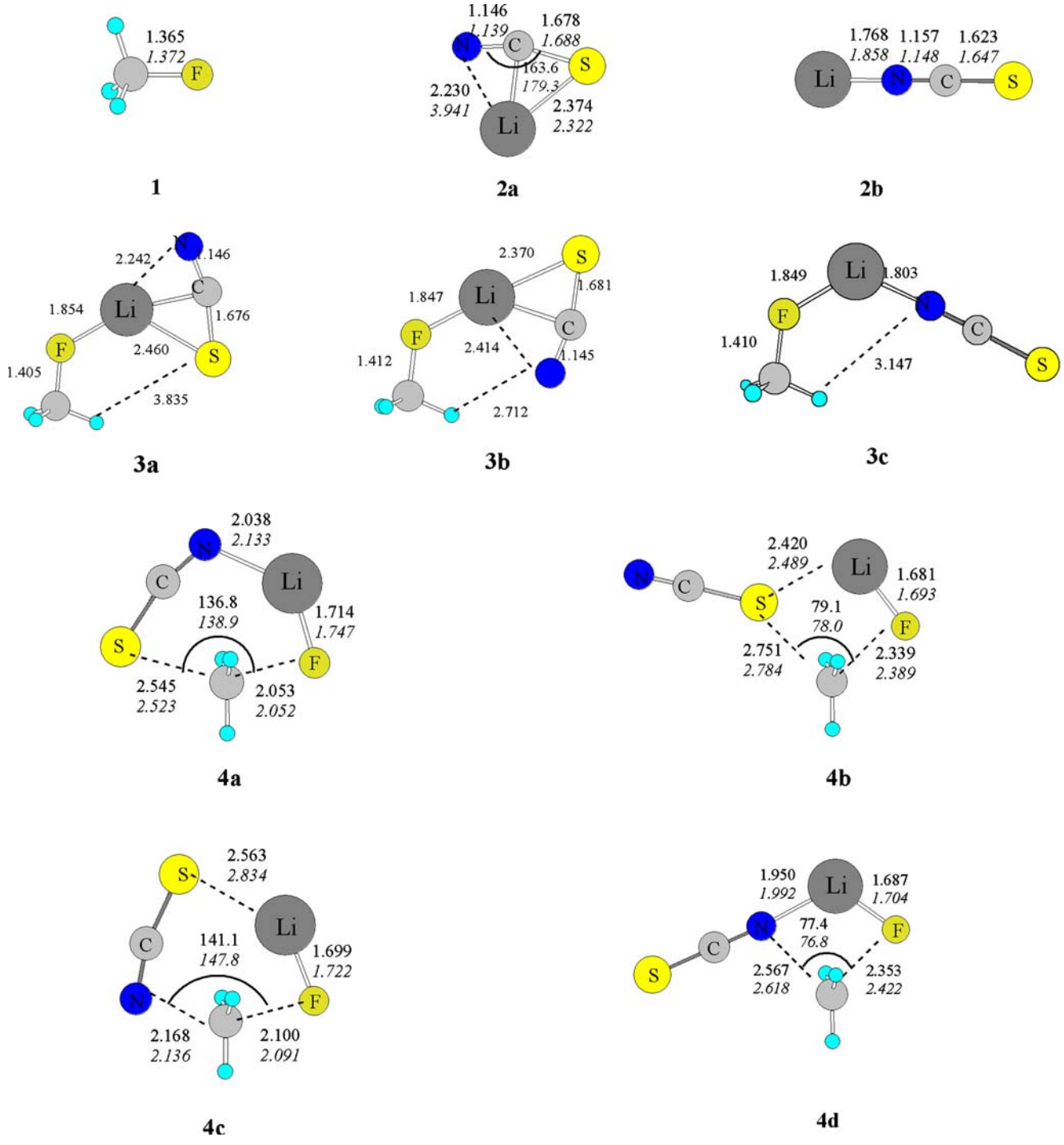

Fig. 1 Selected HF/6-311 + G** optimized geometries of all species involved in the reaction LiNCS + CH3F in the gas phase (*in regular*) and in CH_3COCH_3 (*in italic*), respectively

4c′ are substantially larger than for TS (**4a** and **4c**) with inversion of configuration and the barrier for four-membered-ring retention TS structures **4b′** and **4d′** are substantially lower than the corresponding barrier in the inversion TS **4b** and **4d**, respectively. We can explain these phenomena by comparing the geometrical characteristics of the TS structures. In the six-membered-ring retention TS structures, the bridging action of the lithium cation causes remarkable deformations in **4a′** and **4c′** relative to the inversion TS geometries (**4a** and **4c**). The smaller S–C–F or N–C–F angles (decreasing from ~140° in **4a** and **4c** to ~80° in **4a′** and **4c′**) and short N–F and S–F distances will increase the repulsion between nucleophilic site and the leaving group, therefore destabilize the retention TS structures. However, in the four-membered-ring inversion TS structures (**4b** and **4d**)

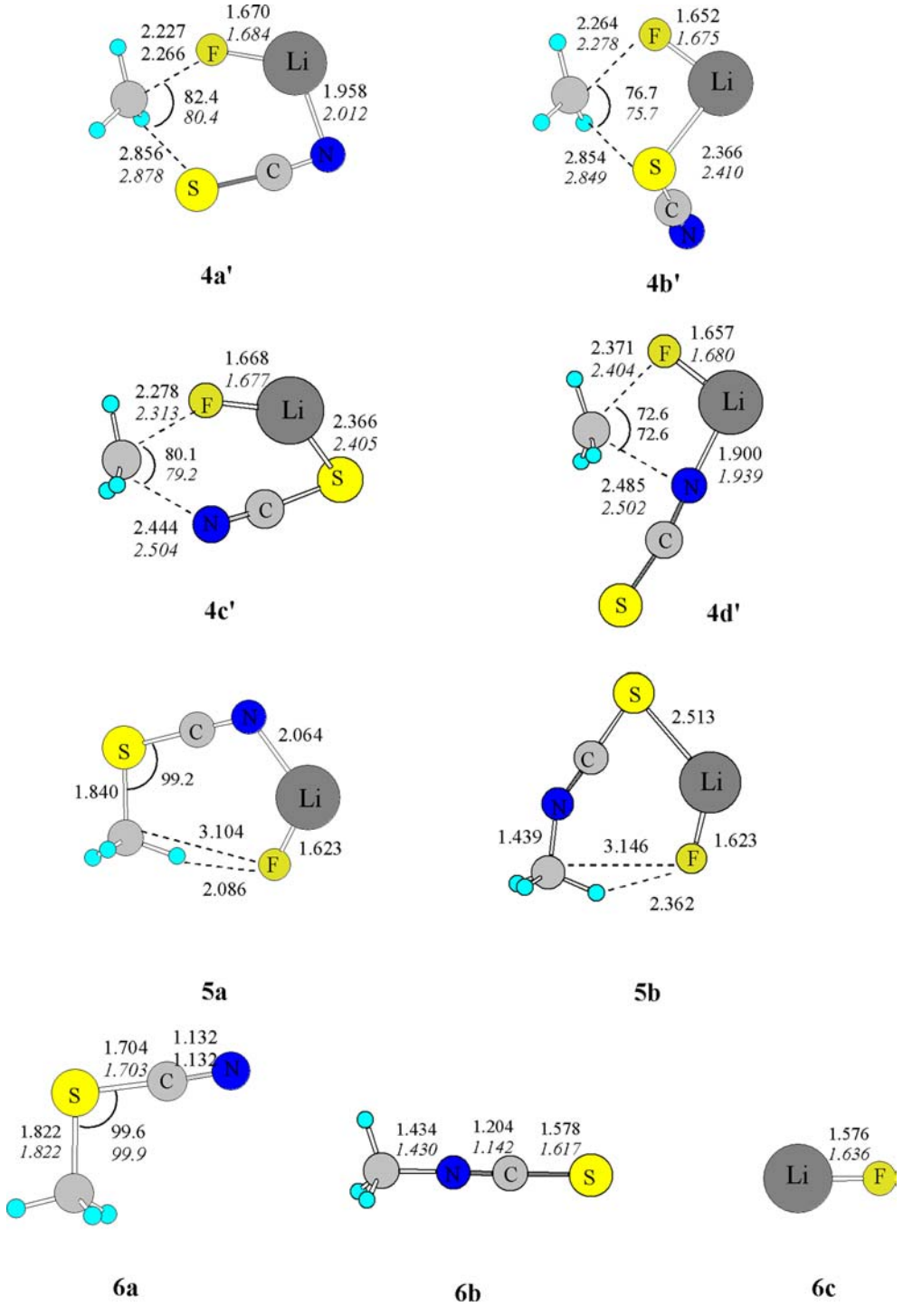

Fig. 1 (Contd.)

and the retention TS structures (**4b′** and **4d′**), the S–C–F or N–C–F angles are almost the same (~80°). The shorter C–F and Li–F distances in **4b′** and **4d′** stabilize these retention TS structures and lower the reaction barrier. The energy analysis in Table 1 shows that **4a** is clearly the best transition structure and methyl thiocyanate CH_3SCN should be the initial product in the title gas phase reaction with the inversion mechanism. On the other hand, the initial product will be methyl isothiocyanate if the ion-pair reaction involves the retention mechanism.

Exploring reaction pathways

Based on the calculated MP2(full) potential energy surface and IRC analysis, the eight possible reaction pathways in the gas phase reaction (Eq. 2) are proposed

Table 1 The MP2(full) relative enthalpies (kJ mol^{-1}), ΔH_{298}(gas), and Gibbs free energies (bold, kJ mol^{-1}), ΔG_{298}(gas), with respect to the reactants at 298.15 K for the reaction of LiNCS with CH_3F in the gas phase

Pathway	Reactants	R-com	Inv-TS	Ret-TS	P-com	Products	
I or V	0.0	−70.8	70.0	159.6	−115.9	−25.7	
LiNCS(l) + CH_3F	**0.0**	**−43.1**	**113.9**	**195.9**	**−79.2**	**−27.4**	CH_3SCN + **6c**
II or VI	0.0	−65.8	254.0	183.3	−112.5	22.3	
LiNCS(T) + CH_3F	**0.0**	**−39.5**	**299.0**	**221.6**	**−72.4**	**−20.6**	CH_3SCN + **6c**
III or VII	0.0	−74.7	120.5	176.8	−111.7	−26.8	
LiNCS(T) + CH_3F	**0.0**	**−42.3**	**165.8**	**214.5**	**−71.6**	**−25.5**	CH_3NCS + **6c**
IV or VIII	0.0	−70.8	214.4	162.3	−115.1	−30.2	
LiNCS(l) + CH_3F	**0.0**	**−43.1**	**250.6**	**197.4**	**−78.4**	**−32.3**	CH_3NCS + **6c**

Table 2 The MP2(full) overall barriers and the overall energy change (kJ mol^{-1}) in the title reaction (Eq. 2) in CH_3COCH_3 solution at 298.15 K

Pathway	$\Delta H^{\neq}_{298}$(sol)		$\Delta G^{\neq}_{298}$(sol)		ΔH_{298}(sol)	ΔG_{298}(sol)
	Inv.	Ret.	Inv.	Ret.		
I or V	299.0	405.6	342.9	441.9	−36.4	−38.1
II or VI	294.6	269.2	339.6	307.5	−137.6	−135.9
III or VII	215.9	318.5	261.2	356.3	−136.7	−135.5
IV or VIII	424.5	428.0	460.7	463.2	−35.5	−37.6

as follows, in which I–IV proceed via the inversion mechanism, while V–VIII by the retention mechanism (Table a).

It is shown that more favorable reaction channels in the gas phase for the title reaction are those involving six-membered-ring inversion TS structures, in which pathway I, passing through inversion TS (**4a**) to reach the product CH_3SCN (**6a**), is the most kinetically favorable. More stable methyl isothiocyanate CH_3NCS can be prepared by the rearrangement of CH_3SCN.

Charge distributions

The geometrical characteristics of TS and the reaction barriers can be investigated further by a study of the charge distributions based on the NPA of Reed and Weinhold [28]. The results are summarized in Table 3 for the inversion transition structures, **4a**–**d**, and in Table 2 for the retention transition structures, **4a′**–**d′**. Tables 2 and 3 also include the total "group charges" on the methyl group by adding the contributions of the component atoms.

The NPA for all TS structures reveal considerable positive charges on the methyl groups (+0.603 to +0.888), which suggests that the organic moiety has typical carbocation character. Thus, the ion-pair S_N2 transition states can be modeled as an anion, $FLiNCS^-$ or $FLiSCN^-$, interacting with a methyl cation. Thus, our conclusions support the mechanism of the carbocation S_Ni type proposed by Harder et al. [12] for the reaction of CH_3F with LiF.

Charge distributions in Tables 3 and 4 also show that the leaving fluorine atom bears lower negative charge in **4a** (−0.229) and **4c** (−0.568), but higher in **4b** (−0.931) and **4d** (−0.929). These charges on the F atom can be related with the S_N2 reaction barriers. Generally speaking, in the S_N2 reaction, the more the electrons on the same leaving group, the later the transition state, the higher the reaction barrier, which is consistent with the results in Table 1. The overall barriers, $\Delta G^{\neq}_{298}$(gas), for the reaction pathways via TS **4b** (299.0 kJ mol^{-1}) or **4d** (250.6 kJ mol^{-1}) are higher than the others. The charges on F atom in **4a′**-**d′** (−0.863 ∼ −0.921) are between **4a, 4c** and **4b, 4d**, so the $\Delta G^{\neq}_{298}$(gas) values for **4a′**-**d′** (195.9 ∼ 221.6 kJ mol^{-1}) are higher than **4a** and **4c**, lower than **4b** and **4d**.

Solvation effects

As shown in Fig. 1, some of structural parameters of species in Eq. 2 change significantly on going from the gas phase to polar solution and therefore large effects on solvation free energies are to be expected. The main geometrical modifications induced by CH_3COCH_3 are the lengthening of the Li–N, Li–S and Li–F distances, which leads to looser TS state structures in solution. Another important solvent effect is the increase of angle N–C–S in **2a** from 163.6 to 179.3°. We were unable to locate the stable structures for all complexes (**3a**–**c** and **5a**–**b**) in CH_3COCH_3. This points to an interesting problem for further study, but it does not affect the following discussion about the kinetics and thermodynamics of the title reaction in polar solution.

Solvent effects on the total Gibbs free energies for all species, kinetic and thermodynamic parameters in the title reaction are compiled in Tables 5 and 2, respectively. The relative enthalpies and Gibbs free energies in CH_3COCH_3 were computed at the MP2(full) level using the following equations:

$$\Delta H_{298}(\text{sol}) = \Delta H_{298}(\text{gas}) + \Delta SSE \quad (6)$$

$$\Delta G_{298}(\text{sol}) = \Delta G_{298}(\text{gas}) + \Delta SSE \quad (7)$$

I	LiNCS(l)(**2b**) + CH_3F → R-com3(**3c**) → inv-TS1(**4a**) → P-com1(**5a**) → CH_3SCN(**6a**) + LiF
II	LiNCS(T)(**2a**) + CH_3F → R-com1(**3a**) → inv-TS2(**4b**) → P-com1(**5a**) → CH_3SCN(**6a**) + LiF
III	LiNCS(T)(**2a**) + CH_3F → R-com2(**3b**) → inv-TS3(**4c**) → P-com2(**5b**) → CH_3NCS(**6b**) + LiF
IV	LiNCS(l)(**2b**) + CH_3F → R-com3(**3c**) → inv-TS4(**4d**) → P-com2(**5b**) → CH_3NCS(**6b**) + LiF
V	LiNCS(l)(**2b**) + CH_3F → R-com3(**3c**) → ret-TS1(**4a'**) → P-com1(**5a**) → CH_3SCN(**6a**) + LiF
VI	LiNCS(T)(**2a**) + CH_3F → R-com2(**3b**) → ret-TS2(**4b'**) → P-com1(**5a**) → CH_3SCN(**6a**) + LiF
VII	LiNCS(T)(**2a**) + CH_3F → R-com2(**3b**) → ret-TS3(**4c'**) → P-com2(**5b**) → CH_3NCS(**6b**) + LiF
VIII	LiNCS(l)(**2b**) + CH_3F → R-com3(**3c**) → ret-TS4(**4d'**) → P-com2(**5b**) → CH_3NCS(**6b**) + LiF

Table 3 MP2(full) natural population analysis (NPA) charges of the four retention transition structures (**4a′-d′**)

Atom	**4a′**	**4b′**	**4c′**	**4d′**
C1[a]	0.20278	0.19104	0.28177	0.2343
H	0.18405	0.19034	0.19169	0.18094
H	0.17708	0.18252	0.18225	0.18095
H	0.20543	0.21058	0.20459	0.23396
F	−0.90626	−0.90952	−91968	−0.9206
Li	0.9563	0.93742	0.93056	0.95806
N	−0.68234	−0.45245	−64071	−0.84309
C2[b]	0.21586	0.09501	0.21669	0.24276
S	−0.3529	−0.44493	−44716	−0.2673
CH_3^c	0.76934	0.77448	0.8603	0.83015

[a]on the CH_3 moiety
[b]on the NCS moiety
[c]Group charge obtained by summing component carbon (C1) and three hydrogen atoms

Table 4 MP2(full) natural population analysis (NPA) charges of the four inversion transition structures (**4a (d**)

Atom	**4a**	**4b**	**4c**	**4d**
C1[a]	0.03667	0.27322	0.13445	0.32359
H	0.18433	0.15173	0.18881	0.14679
H	0.19077	0.20842	0.19009	0.20862
H	0.19077	0.20842	0.19009	0.20862
F	−0.22913	−0.93105	−0.56774	−0.92947
Li	0.95451	0.94653	0.92641	0.95441
N	−0.85425	−0.56904	−0.87116	−0.8911
C2[b]	0.21447	0.1364	0.22683	0.26163
S	−0.68815	−0.42463	−0.41779	−0.28309
CH_3^c	0.60254	0.84179	0.70344	0.88762

[a]on the CH_3 moiety
[b]on the NCS moiety
[c]Group charge obtained by summing component carbon (C1) and three hydrogen atoms

The data in Table 2 show that the title reaction will be significantly retarded in CH_3COCH_3 solution, which might be taken as a reflection of stronger solvation of the original reactants relative to the TS structures. The reactant **2a** and its isomer **2b** have larger dipole moments than eight possible TS structures with smaller dipole moments (less than 10.0 D). The decrease in dipole moment accompanying this reaction implies that a polar solvent should be able to retard the reaction more than a non-polar solvent. The reaction barriers in polar CH_3COCH_3 solution are much higher than those in the gas phase, increasing in a different order in terms of $\Delta G^{\neq}_{298}$(sol): 261.2(**4c**) < 307.5(**4b′**) < 339.6(**4b**) < 342.9(**4a**) < 356.3(**4c′**) < 441.9(**4a′**) < 460.7(**4d**) <

Table 5 Calculated total energies (Hartree) in the gas phase, dipole moments (D) in CH_3COCH_3 and solvent stabilization energies (kJ mol^{-1}) for species involved in the exchange reaction LiNCS + CH_3F

	MP2(full)/6-311 + G//HF/6-311 + G****		**μ(sol)**	**SSE**
	H_{298}(gas)	G_{298}(gas)		
CH_3F (**1**)	−139.451664	−139.476875	2.34	−9.3
LiNCS(T) (**2a**)	−497.975113	−498.006700	11.93	−228.3
LiNCS(l) (**2b**)	−497.973813	−498.004113	13.39	−333.0
R-com1 (**3a**)	−637.451855	−637.498610		
R-com2 (**3b**)	−637.455227	−637.499668		
R-com3 (**3c**)	−637.452448	−637.497397		
inv-TS1 (**4a**)	−637.398807	−637.437605	2.96	−113.2
inv-TS2 (**4b**)	−637.330045	−637.369683	9.03	−197.0
Inv-TS3 (**4c**)	−637.380885	−637.420441	4.27	−142.2
inv TS4 (**4d**)	−637.343809	−637.385534	6.78	−132.2
ret-TS1 (**4a'**)	−637.364683	−637.406365	7.50	−96.2
ret-TS2 (**4b′**)	−637.356982	−637.399173	6.15	−151.7
ret-TS3 (**4c′**)	−637.359439	−637.401874	7.56	−95.9
ret TS4 (**4d′**	−637.363670	−37.405805	5.61	76.5
P-com1 (**5a**)	−637.469620	−637.511146		
P-com2 (**5b**)	−637.469318	−637.510831		
CH_3SCN (**6a**)	−530.195139	−530.228580	5.13	−48.7
CH_3NCS (**6b**)	−530.196872	−530.230449	6.26	−43.3
LiF (**6c**)	−107.240119	−107.262857	7.28	−304.2

463.2(**4b**) kJ mol^{-1}. The most intriguing point is that the overall barrier for TS **4c** (in path III) is lower than **4a** in path I by 46.3 kJ mol^{-1}. Thus, the thermodynamically favorable CH_3NCS will be the product if the reaction of LiNCS with CH_3F occurs in CH_3COCH_3 solution, which can be explained by the fact that the linear **2b** (13.39 D) is more stable than the T-shaped isomer **2a** (11.93 D) by 97.9 kJ mol^{-1}, and TS **4c** (4.27 D) is more solvated than **4a** (2.96 D) in CH_3COCH_3.

Conclusions

Application of MP2(full) theory to the ion-pair S_N2 reaction of lithium isothiocyanate with methyl fluoride in the gas phase and in CH_3COCH_3 solution leads to the following conclusions:

(1) For the title reaction in the gas phase, eight possible reaction pathways are predicted, including inversion (I–VI) and retention mechanisms (V–VIII).
(2) In the gas phase, the six-membered-ring inversion transition structures (**4a** and **4c**) are much lower in energy than the others (**4b** and **4d**). All retention transition structures have similar energies (within 26 kJ mol^{-1}), in which **4a′** and **4d′** are more stable than the other two (**4b′** and **4c′**). Methyl thiocyanate CH_3SCN should preferentially form no matter whether the reaction follows the inversion mechanism or retention mechanism.
(3) Solvent effects will significantly affect the geometries of species containing polar Li–N and Li–S bonds, and the rate of the title reaction will be retarded due to the larger free energies of solvation for the reactant LiNCS. The most favorable reaction pathway (III) in CH_3COCH_3 will lead to the more stable product CH_3NCS.
(4) Comparison of the two mechanisms shows that the inversion mechanism is more favorable both in the gas phase and in solution.

Acknowledgements This work was funded by the Science Foundation of Chongqing City, PRC (Grant No.2002-7473). We thank a referee for helpful comments and references.

References

1. Guy G (1977) The chemistry of cyanates and their thio derivatives. In: Patai S (ed) Wiley, London, (Chap. 18, and references cited therein)
2. Wilson LJ (2001) Org Lett 3:585–588
3. Rydberg P, Luning B, Wachtmeister CA, Eriksson L, Tornqvist M (2002) Chem Res Toxicol 15:570–581
4. Evindar G, Batey RA (2003) Org Lett 5:1201–1204
5. D'hooghe M, Waterinckx A, De Kimpe N (2005) J Org Chem 70:227–232
6. Shaker RM, Mahmoud AF, Abdel-Latif FF (2005) Phosphorus Sulfur 180:397–406
7. Smith PAS, Emerson DW (1960) J Am Chem Soc 82:3076–3081
8. Cremlyn RJ (1996) An introduction to organosulfur chemistry. Wiley Chichester, UK, pp 142–143
9. Shaik SS, Schlegel HB, Wolfe S (1992) Theoretical aspects of physical organic chemistry, the S_N2 mechanism. Wiley, New York
10. Laerdahl JK, Uggerud E (2002) Int J Mass Spectrom 214:277–314 (and references cited therein)
11. Gonzales JM, Pak C, Cox S, Allen WD, Schaefer III HF, Csäszár AG, Tarczay G (2003) Chem Eur J 9:2173–2192
12. Harder S, Streitwieser A, Petty JT, Schleyer PvR (1995) J Am Chem Soc 117:3253–3259
13. Streitwieser A, Choy GSC, Abu-Hasanayn F (1997) J Am Chem Soc 119:5013–5019
14. Leung SSW, Streitwieser A (1998) J Comput Chem 19:1325–1336
15. Ren Y, Chu SY (2004) J Comput Chem 25:461–471
16. Ren Y, Chu SY (2004) J Phys Chem A 108:7079–7086
17. Winstein S, Savedoff LG, Smith S, Stevens IDR, Gall JS (1960) Tetrahedron Lett 24–30
18. Cayzergues P, Georgoulis C, Mathieu GJ (1987) Chim Phys Phys Chim Biol 84:63–70
19. Westaway KC, Waszczylo Z, Smith PJ, Rangappa KS (1985) Tetrahedron Lett 26:25–28
20. Westaway KC, Lai ZG (1988) Can J Chem 66:1263–1271
21. Westaway KC, Lai ZG (1989) Can J Chem 67:345–349
22. Lai ZG, Westaway KC (1989) Can J Chem 67:21–26
23. Zhu HJ, Ren Y, Ren J, Chu SY (2005) Int J Quantum Chem 101:104–112
24. Glukhovtsev MN, Pross A, Schlegel HB, Bach RD, Radom L (1996) J Am Chem Soc 118:11258–11264
25. Xiong Y, Zhu HJ, Ren Y (2003) J Mol Struct (THEOCHEM) 664–665:279–289
26. Veszprémi T, Pasinszki T, Feher M (1994) J Am Chem Soc 116:6303–6306
27. Scott AP, Radom L (1996) J Phys Chem 100:16502–16513
28. Gonzalez C, Schlegel HB (1989) J Chem Phys 90:2154–2161
29. Gonzalez C, Schlegel HB (1990) J Chem Phys 94:5523–5527
30. Reed AE, Weinstock RB, Weinhold F (1985) J Chem Phys 83:735–746
31. Tomasi J, Persico M (1994) Chem Rev 94:2027–2094
32. Frisch MJ, Trucks GW, Schlegel HB, Scuseria GE, Robb MA, Cheeseman JR, Zakrzewski VG, Montgomery JA, Stratman RE, Burant JC, Dapprich S, Millam JM, Daniels AD, Kudin KN, Strain MC, Farkas O, Tomasi J, Barone V, Cossi M, Cammi R, Mennucci B, Pomelli C, Adamo C, Clifford S, Ochterski J, Petersson GA, Ayala PY, Cui Q, Morokuma K, Malick DK, Rabuck AD, Raghavachari K, Foresman JB, Cioslowski J, Ortiz JV, Baboul AG, Stefanov BB, Liu C, Liashenko A, Piskorz P, Komaromi, I, Gomperts R, Martin RL, Fox DJ, Keith T, Al-Laham MA, Peng CY, Nanayakkara A, Gonzalez C, Challacombe M, Gill PMW, Johnson BG, Chen W, Wong MW, Andres JL, Gonzales C, Head-Gordon M, Replogle ES, Pople JA (1998) Gaussian 98, Revision A.9. Gaussian Inc, Pittsburgh, PA
33. Kotani M, Shigetomi Y, Imada M, Ōki M, Nagaoka M (1997) Heteroatom Chem 8:35–43